

# Identification of Scanning Slit-Beam Topographic Parameters Important in Distinguishing Normal from Keratoconic Corneal Morphologic Features

BARIS SONMEZ, MD, MINH-PHUONG DOAN, MD, AND D. REX HAMILTON, MD, MS

- **PURPOSE:** To identify morphologic parameters obtained using scanning slit-beam topography that help distinguish normal from keratoconic corneal morphologic features.
- **DESIGN:** Observational, retrospective, cross-sectional study.
- **METHODS:** This retrospective review examined 207 normal eyes of patients undergoing an initial consultation for primary refractive surgery and 42 eyes with clinical keratoconus (KCN). The following parameters were examined and compared between the two groups: astigmatism, central corneal power, irregularity indices at 3 mm (II3) and 5 mm (II5), maximal posterior elevation (MPE) magnitude and location, thinnest optical pachymetry (TOP) magnitude and location, anterior elevation best-fit sphere (ABFS), posterior elevation best-fit sphere (PBFS), the ratio of ABFS to PBFS, the difference between average inferior and average superior K values at 3 mm and 5 mm in both keratometric (I-S K3 and I-S K5) and tangential (I-S T3 and I-S T5) topographic maps, and skewed radial axis at 3 mm (SRAX3) and 5 mm (SRAX5) of the keratometric topography map.
- **RESULTS:** The II3, II5, MPE magnitude, TOP magnitude, ABFS, PBFS, ABFS-to-PBFS ratio, I-S K at both 3 mm and 5 mm, I-S T at both 3 and 5 mm, and SRAX at 3 mm and 5 mm values were significantly different among the two groups ( $P < .001$ ). The least-correlated parameters were SRAX3, TOP magnitude, and II3 in the KCN group and I-S K3, amount of astigmatism and MPE magnitude in the normal group.
- **CONCLUSIONS:** Parameters obtained using scanning slit-beam topography may allow improved differentiation

of keratoconic from normal corneal shapes, especially when the poorly correlated intragroup parameters are used. (Am J Ophthalmol 2007;143:401-408. © 2007 by Elsevier Inc. All rights reserved.)

**L**ASER IN SITU KERATOMILEUSIS (LASIK) IS THE METHOD of laser vision correction preferred both by patients and most surgeons because of rapid visual recovery, minimal discomfort, high predictability, and excellent safety profile.<sup>1,2</sup> This procedure is not without risk, however, and rarely can result in devastating vision loss, an extremely unsatisfactory result from an elective procedure on an eye with excellent preoperative best-corrected vision.<sup>3</sup>

Corneal ectatic disorders, such as keratoconus (KCN) and pellucid marginal degeneration (PMD), are well-accepted contraindications for LASIK surgery.<sup>4-6</sup> Diagnosis of manifest KCN is made by clinical observation: angulation of the lower lid in downgaze (Munson sign), scissoring of the retinoscopic reflex, asymmetric corneal thinning, an iron line surrounding the cone (Fleischer ring), and stress lines in the area of the cone (Vogt striae). Corneal topography is helpful in confirming the diagnosis in patients with manifest KCN.

Forme fruste keratoconus (FFKCN), or subclinical KCN, occurs in patients with none of the above clinical findings and good best-corrected visual acuity but abnormal corneal topography. Forme fruste KCN also is considered a contraindication for LASIK surgery because it is hypothesized that the creation of the LASIK flap and excimer ablation of the corneal stroma cause a mechanical weakening of the cornea that could convert an FFKCN cornea into a manifest KCN cornea.<sup>7,8</sup> Although photorefractive keratectomy (PRK) has been investigated as a surgical treatment option for FFKCN patients,<sup>9</sup> it does not eliminate the risk for postsurgical ectasia, even in cases of low myopic correction.<sup>10</sup>

Post-LASIK ectasia is a devastating complication that occurs after LASIK surgery and is characterized by refrac-

Accepted for publication Nov 3, 2006.

From The Jules Stein Eye Institute, David Geffen School of Medicine at the University of California, Los Angeles, Los Angeles, California.

Inquiries to D. Rex Hamilton, MD, MS, UCLA Laser Refractive Center, Department of Ophthalmology, Division of Cornea/External Disease, The Jules Stein Eye Institute, 100 Stein Plaza, UCLA, Los Angeles, CA 90095; e-mail: hamilton@jsei.ucla.edu

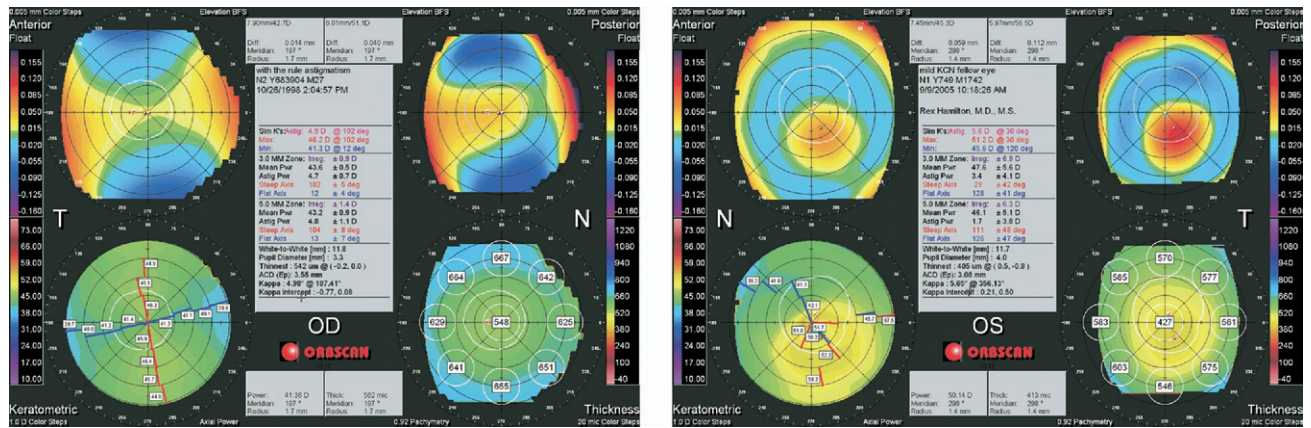


**FIGURE 1.** Example of Orbscan topography of (Left) a normal and (Right) a keratoconic cornea. (Top left) anterior elevation, (Top right) posterior elevation, (Bottom left) keratometric map, (Bottom right) optical pachymetry. A few of the important differences to note are: (1) maximum posterior elevation: normal, 40  $\mu\text{m}$ ; keratoconus (KCN), 112  $\mu\text{m}$ ; (2) irregularity index at 3 mm: normal, 0.9 diopters (D); KCN, 6.9 D; (3) thinnest optical pachymetry: normal, 542  $\mu\text{m}$ ; KCN, 405  $\mu\text{m}$ ; (4) skewing of the superior and inferior radial axis of astigmatism: normal, absent or minimal skewing; KCN, significant skewing.

tive instability associated with a corresponding progressive structural deformation of the cornea. Indices based on anterior corneal topographic findings have been developed to detect FFKCN.<sup>11-13</sup> In addition to FFKCN, other risk factors for post-LASIK ectasia include preoperative corneal thickness <500  $\mu\text{m}$ , high myopic corrections with a residual bed thickness of less than 250  $\mu\text{m}$ , and an unexpectedly thick LASIK flap.<sup>7,14,15</sup> Although the surgeon ultimately has control over the LASIK parameters and decides whether to proceed or defer surgery, some patients with normal anterior topographic findings and modest excimer laser ablations unfortunately have gone on to experience post-LASIK ectasia.<sup>16-19</sup>

Orbscan (Bausch & Lomb, Salt Lake City, Utah, USA) scanning slit-beam topography is a commonly used device in refractive surgery screening because it provides information from both the anterior corneal surface and the posterior corneal surface as well as corneal thickness measurements across the entire cornea.<sup>20-22</sup> Although the Orbscan system provides the surgeon with a myriad of morphologic parameters to describe the cornea, we are unaware of any systematic study examining which of these parameters are most useful in differentiating normal from abnormal (e.g., KCN) corneal morphologic features (Figure 1).<sup>23</sup> The main purpose of this study, therefore, was to identify those parameters obtained from scanning slit-beam topography that are most useful in distinguishing normal from abnormal corneal morphologic features.

## METHODS

THE RESEARCHERS FOLLOWED THE TENETS OF THE DECLARATION OF Helsinki in the treatment of the patients reported herein. Study approval was obtained from the Institutional

Review Board at The University of California, Los Angeles (UCLA M-IRB no. G05-12-059-01).

Orbscan IIz measurements were evaluated retrospectively for two groups. Group 1 included patients who underwent refractive surgery screening and had normal corneal examination findings. Group 2 included patients with KCN who had at least one of the clinical findings of manifest KCN: The Fleischer ring, Vogt striae, Munson sign, or scissoring of the retinoscopic reflex combined with irregular astigmatism.

All of the Orbscan measurements were performed by experienced technicians using an acquisition protocol recommended by the manufacturer. Images of poor quality (e.g., missing data points, poor fixation, lid artifacts) were discarded. Patients with dry eyes or corneal scars and those who underwent previous ocular surgery were excluded. Default settings for best-fit spheres were used in all cases: floating alignment and full cornea fit zone (10 mm). The center of all maps was the apex determined by Placido data. The following quantitative indices from the Orbscan measurements were analyzed: amount of astigmatism (A) in diopters (D), central corneal power in diopters (CKP), anterior elevation best-fit sphere (ABFS), posterior elevation best-fit sphere (PBFS), and the ratio of ABFS to PBFS.

- **IRREGULARITY INDICES AT 3 mm AND 5 mm:** Irregularity indices at 3 mm (II3) and 5 mm (II5) show the optical surface irregularity that is proportional to the standard deviation of the axis-independent surface curvature. They are calculated automatically from within the Orbscan IIz software according to a statistical combination of the standard deviations of the mean and toric curvatures.<sup>24</sup>
- **MAXIMUM POSTERIOR ELEVATION:** The maximum posterior elevation (MPE) is the absolute magnitude in

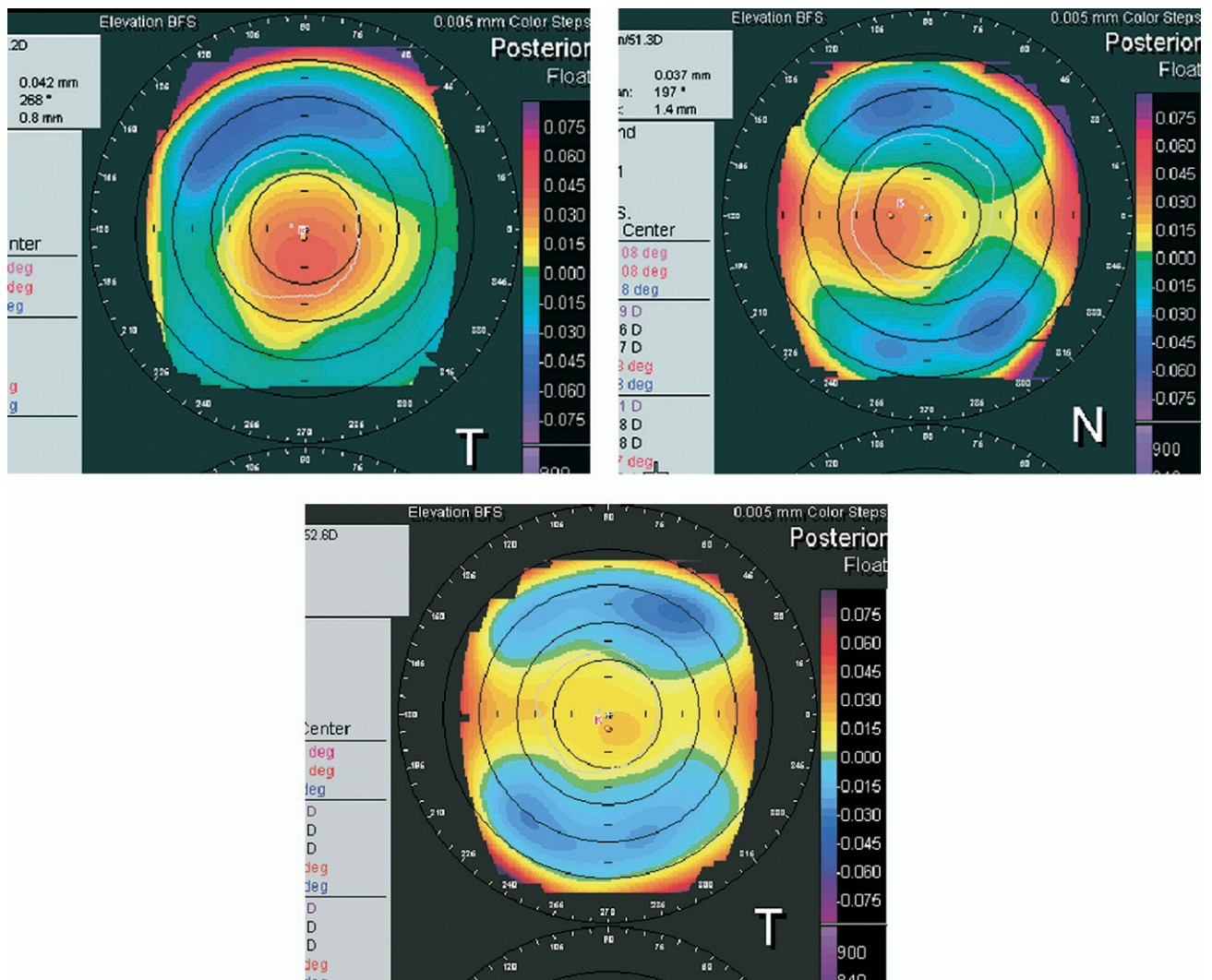


FIGURE 2. Determination of maximum posterior elevation (MPE). (Top left and right) Island: MPE occurs within the central 5 mm and is surrounded by concentric zones of decreasing elevation. (Bottom) Regular ridge: central elevation that increases uniformly and monotonically in the opposite directions to corneal periphery. In this case, the very center of the posterior corneal elevation map is chosen as the MPE.

micrometers ( $\mu\text{m}$ ) of the posterior corneal surface above the best-fit sphere. Default settings of Orbscan IIz for best-fit sphere were used in all measurements. Vector location in polar coordinates included the meridian (degrees) and radius (distance from the central cornea in millimeters). The meridional location of the MPE was standardized among right and left eyes by transformation using the following formulas for the left eyes: for locations above the horizontal meridian, corrected meridian =  $180 - \text{meridian}$ ; for locations below the horizontal meridian, corrected meridian =  $180 + (360 - \text{meridian})$ . If radius = 0, then the meridian values in either eye were assigned as 0. Determination of the MPE location was as follows: island (Figure 2, Top left and right), maximum posterior elevation occurs within the central 5 mm and is surrounded by concentric zones of decreasing elevation; regular ridge (Figure 2, Bottom),<sup>20</sup> central elevation that

TABLE 1. Demographic Data of Normal and Keratoconic Eyes

Characteristics	Normal Eyes	Keratoconic Eyes
No. of patients	108	24
Male gender	54 (50%)	18 (75%)
Age (yrs), mean $\pm$ SD	39 $\pm$ 11	41 $\pm$ 10
No. of eyes	207	42
Mean spherical equivalent (D)	-3.56	-3.82

D = diopters; SD = standard deviation.

increases uniformly and monotonically in opposite directions to corneal periphery. In this patient, the very center of the posterior corneal elevation map was chosen as the MPE because the peripheral elevation was

**TABLE 2.** Comparison of Scanning Slit-Beam Topographic Indices between Normal and Keratoconic Eyes

Orbscan Indices	Present Study			Wei and associates <sup>20</sup> ; Normal Eyes
	Normal Eyes	KCN Eyes	P value*	
Amount of astigmatism (D)	1.02 ± 0.85	3.62 ± 2.60	<.0001	1.18 ± 0.86
Central corneal power (D)	43.42 ± 6.88	49.22 ± 5.53	<.0001	44.5 ± 1.5
Irregularity index 3 mm	1.04 ± 0.33	4.20 ± 2.15	<.0001	1.07 ± 0.35
Irregularity index 5 mm	1.33 ± 0.36	4.50 ± 2.44	<.0001	1.40 ± 0.37
MPE magnitude (μm)	28.2 ± 7.1	81.2 ± 36.1	<.0001	28 ± 7
MPE meridian (degrees)	210 ± 84	238 ± 35	.0005	NA
MPE radius (mm)	1.12 ± 0.75	1.11 ± 0.41	.900	NA
TOP magnitude (μm)	548 ± 35	472 ± 57	<.0001	553 ± 25
TOP meridian (degrees)	204 ± 78	216 ± 52	.211	NA
TOP radius (mm)	0.71 ± 0.45	0.85 ± 0.32	.021	NA
ABFS (mm)	7.86 ± 0.24	7.68 ± 0.34	.002	7.87 <sup>†</sup>
PBFS (mm)	6.51 ± 0.25	6.25 ± 0.35	<.0001	6.38 <sup>‡</sup>
Ratio ABFS/PBFS	1.21 ± 0.03	1.23 ± 0.03	<.0001	NA
I–S K 3 mm	0.18 ± 0.32	3.24 ± 3.36	<.0001	NA
I–S K 5 mm	0.34 ± 0.42	4.14 ± 3.83	<.0001	NA
I–S T 3 mm	0.41 ± 0.64	6.56 ± 6.16	<.0001	NA
I–S T 5 mm	0.67 ± 1.00	3.94 ± 3.06	<.0001	NA
SRAX 3 mm	34.6 ± 39.1	64.5 ± 41.8	<.0001	NA
SRAX 5 mm	39.5 ± 42.6	81.0 ± 38.3	<.0001	NA

ABFS = anterior best-fit sphere; D = diopters; I–S K = inferior – superior difference in keratometric map; I–S T = inferior – superior difference in tangential map; KCN = keratoconus; MPE = mean posterior elevation; NA = not available; PBFS = posterior best-fit sphere; SRAX = skewed radial axis; TOP = thinnest optical pachymetry. Orbscan is manufactured by Bausch & Lomb, Salt Lake City, Utah, USA.

\*Analysis of variance.

<sup>†</sup>42.8 ± 1.3.

<sup>‡</sup>52.9 ± 1.8; published diopter values<sup>20</sup> were converted to millimeters by the authors for comparison.

a nonpathologic manifestation of normal corneal astigmatic shape.

• **THINNEST OPTICAL PACHYMETRY:** The thinnest optical pachymetry (TOP) is the absolute magnitude in micrometers (μm). The Vector location in polar coordinates was as follows: meridian (degrees) and radius (distance from the central cornea in millimeters). The meridional location of the TOP was standardized among right and left eyes by transformation using the following formulas for the left eyes: for locations above the horizontal meridian, corrected meridian = 180–meridian; for locations below the horizontal meridian, corrected meridian = 180+(360–meridian). If radius = 0, then the meridian values in either eye were assigned as 0.

• **INFERIOR–SUPERIOR DIFFERENCE:** Determination of inferior–superior (I–S) difference for the keratometric map was as follows: K powers at five different locations above (30, 60, 90, 120, and 150 degrees) and below (210, 240, 270, 300, and 330 degrees) the horizontal meridian at 3 mm and 5 mm circles were recorded from the keratometric map. The average inferior K power minus the average superior K power at 3 mm (I–S K3) and 5 mm (I–S K5) were calculated. Determination of I–S differ-

ence for the tangential map was as follows: K powers at five different locations above (30, 60, 90, 120, and 150 degrees) and below (210, 240, 270, 300, and 330 degrees) the horizontal meridian at 3 mm and 5 mm circles were recorded from the tangential map. The average inferior K power minus the average superior K power at 3 mm (I–S T3) and 5 mm (I–S T5) were calculated.

• **SKEWING OF THE RADIAL AXIS:** Determination of the skewing of the radial axis (SRAX) was as follows: the location of the steepest keratometric value above and below the horizontal meridian at 3 mm (SRAX3) and 5 mm (SRAX5) of the keratometric map were recorded. The SRAX values were calculated as previously described by Rabinowitz and associates<sup>25</sup>: SRAX = 180–(steep inferior axis–steep superior axis) for 3 mm and 5 mm circles.

All the above data were entered into a Microsoft Excel (Microsoft, Redmond, Washington, USA) spreadsheet, including patient demographic information and manifest refraction.

• **STATISTICAL ANALYSIS:** Statistical analysis was performed using SAS software version 9.1 (SAS Institute, Cary, North Carolina, USA). The differences in all parameters between the KCN and normal groups were

**TABLE 3.** Scanning Slit-Beam Topography Parameters with Strongest Correlations in the Group with Normal Eyes (n = 207)

Indices	r*	P value
I-S T3 and I-S K5	0.877	<.0001
ABFS and PBFS	0.812	<.0001
I-S K3 and I-S K5	0.787	<.0001
I-S K3 and I-S T3	0.752	<.0001
SRAX 3 mm and SRAX 5 mm	0.580	<.0001

ABFS = anterior best-fit sphere; I-S K = inferior – superior difference in keratometric map; I-S T = inferior – superior difference in tangential map; PBFS = posterior best-fit sphere; SRAX = skewed radial axis.

\*Pearson correlation coefficient.

**TABLE 4.** Scanning Slit-Beam Topography Parameters with Weakest Correlations in the Group with Normal Eyes (n = 207)

Indices	r*	P value
I-S K3 and ABFS	-0.0016	.982
ABFS and TOP meridian	-0.0028	.968
I-S K3 and MPE magnitude	-0.0032	.964
MPE magnitude and MPE meridian	-0.0033	.963
I-S T5 and MPE radius	0.0033	.962

ABFS = anterior best-fit sphere; I-S K = inferior – superior difference in keratometric map; I-S T = inferior – superior difference in tangential map; MPE = mean posterior elevation; TOP = thinnest optical pachymetry.

\*Pearson correlation coefficient.

assessed using two-sided Student *t* tests. Pearson correlation coefficients were calculated to evaluate the relationship between parameters within KCN and normal groups. A *P* value < .05 was considered to be statistically significant.

## RESULTS

TWO HUNDRED SEVEN NORMAL EYES OF 108 PATIENTS (50% male, 50% female) who underwent a refractive surgery evaluation (normal group) and 42 eyes of 24 patients (75% male, 25% female; *P* = .026) with clinical KCN (KCN group) were analyzed (Table 1). The mean ages were 39 years in the normal group and 41 years in KCN group. The mean spherical equivalents were -3.56 D for the normal group and -3.82 D for KCN group. The group of normal eyes consisted of 180 myopic (87%), 3 emmetropic (1.4%) and 24 hyperopic (11.6%) eyes.

Table 2 summarizes the means, standard deviations, and *P* values for the various parameters studied in the two

**TABLE 5.** Scanning Slit-Beam Topography Parameters with Strongest Correlations in the Keratoconus Group (n = 42)

Indices	r*	P value
I-S T3 and I-S K5	0.979	<.0001
I-S K3 and I-S K5	0.977	<.0001
I-S K3 and I-S T3	0.970	<.0001
ABFS and PBFS	0.929	<.0001
II3 and II5	0.894	<.0001

ABFS = anterior best-fit sphere; II3 = irregularity index at 3 mm; II5 = irregularity index at 5 mm; I-S K = inferior – superior difference in keratometric map; I-S T = inferior – superior difference in tangential map; PBFS = posterior best-fit sphere.

\*Pearson correlation coefficient.

**TABLE 6.** Scanning Slit-Beam Topography Parameters with Weakest Correlations in the Keratoconus Group (n = 42)

Indices	r*	P value
SRAX3 and TOP magnitude	-0.0030	.985
SRAX3 and II3	0.0057	.972
SRAX5 and TOP meridian	-0.0059	.971
A and TOP meridian	0.0095	.952
I-S T5 and CKP	0.0210	.895

A = ; CKP = central corneal power in diopters; II3 = irregularity index at 3 mm; I-S T = inferior – superior difference in tangential map; SRAX = skewed radial axis; TOP = thinnest optical pachymetry.

\*Pearson correlation coefficient.

groups. The mean values for the amount of astigmatism, central corneal power, and irregularity indices at 3 mm and 5 mm were significantly higher in the KCN group (*P* < .0001). The mean values for the MPE were 28.2 μm in the normal group and 81.2 μm in the KCN group, a highly statistically significant difference (*P* < .0001). The difference in the MPE meridian also was significant (*P* = .0005), whereas the difference in MPE radius was not. The mean TOP values were 548 μm in the normal group and 472 μm in the KCN group (*P* < .0001). The difference in the TOP radius also was significant (*P* = .021), whereas the difference in TOP meridian was not. The difference in both PBFS and the ratio of ABFS to PBFS between two groups were highly significant (*P* < .0001). There was also a statistically significant difference between the two groups for ABFS (*P* = .002). All parameters regarding I-S differences were statistically significant at 3 mm and 5 mm for both keratometric and tangential maps (*P* < .0001). Skewing of the radial axis also was highly statistically significantly different between the two groups at both the 3 mm and 5 mm zones. The five parameters with the strongest and weakest intragroup correlations are shown in

Tables 3 and 4, respectively (normal group), and in Tables 5 and 6, respectively (KCN group).

## DISCUSSION

CORNEAL ECTASIA AFTER KERATOREFRACTIVE SURGERY IS one of the most feared complications for the refractive surgeon and the patient. We now have more than a decade of experience with LASIK and more than 15 years experience with PRK and surface ablation.<sup>26,27</sup> Through this experience, certain risk factors have been identified, with KCN being one of the most important. Guidelines have been suggested that refractive surgeons should follow to minimize risk of ectasia: avoiding high myopic corrections in corneas that, even before surgery, are thin, leaving a residual stromal bed thickness not less than 250  $\mu\text{m}$ , and using intraoperative pachymetry to detect unexpected flap thickness errors.<sup>7,15,28</sup> Despite adherence to these guidelines, cases of ectasia after keratorefractive surgery are still reported, even in cases of low myopic correction.<sup>7,14,16,17</sup>

Keratoconus carries with it an inherent risk of progressive ectasia even without surgery, and therefore is a well-accepted contraindication to LASIK surgery. Subclinical KCN, or FFKCN, remains a difficult entity to identify and likely carries a risk of ectasia after keratorefractive surgery similar to that seen with clinical KCN.<sup>7,29–32</sup> There is little doubt that the introduction of placido disk-based computerized videokeratography increased the surgeon's ability to diagnose some cases of FFKCN and to exclude those patients from candidacy for LASIK surgery.<sup>11–13,33</sup> Because placido disk-based topography systems are limited to providing information about anterior corneal surface morphologic features, scanning slit-beam (Orbscan), rotating Scheimpflug camera-based Pentacam (Oculus Optikgeräte GmbH, Wetzlar, Germany) and Galilei (Ziemer Ophthalmic Systems AG, Port, Switzerland) topography systems were developed. These systems present elevation data from both the anterior and the posterior corneal surface.<sup>34</sup> This elevation-based data also is useful in providing global optical pachymetry information across the entire extent of the cornea.

Scanning slit-beam topography characteristics of normal eyes have been reported.<sup>20–23</sup> Modis and associates<sup>22</sup> evaluated 88 corneas of 44 normal persons and described the corneal curvature characteristics with anterior and posterior curvature mean values and best-fit sphere mean values. Corneal thickness parameters according to different localizations also were presented. Liu and associates<sup>21</sup> reported the results of 94 eyes of 51 normal persons who were examined with Orbscan mainly focusing on corneal thickness parameters and described color-coded patterns in anterior and posterior elevation maps.

The most detailed study to date of Orbscan parameters in normal myopic persons was reported by Wei and associates.<sup>20</sup> They analyzed 140 eyes of 70 normal myopic

persons and described mean values for anterior and posterior best-fit spheres, maximum posterior elevation, thinnest pachymetry, irregularity indices, astigmatism, and keratometry, including correlation between right and the left eyes. No data related to I–S differences or SRAX values were reported. The study group analyzed only myopic eyes, excluding normal corneas with hyperopic refractive error. When the results of the study by Wei and associates are compared with those of our study, striking similarities are noted, particularly in the magnitude of MPE (Table 2). The mean value for MPE was  $28 \pm 7 \mu\text{m}$  in the 100% myopic study group of Wei and associates, with a mean spherical equivalent of  $-5.27 \text{ D}$ .<sup>20</sup> In our study, the mean value for MPE was  $28 \pm 7 \mu\text{m}$  as well. Our normal cohort consisted of 87% myopic eyes with an overall mean spherical equivalent of  $-3.56 \text{ D}$ . In addition, although we did not record the ethnicity of all participants, the normal cohort represents a diverse ethnic mix similar to that of the greater Los Angeles area in which white ethnicity dominates. By contrast, the Wei study group was 94% Asian, with only 6% of participants being White. Thus, despite differences in the refractive and ethnic demographics of the groups in these two studies, the mean maximum posterior elevation magnitude proved to be a very consistent parameter, suggesting that for preoperative screening, the Orbscan device provides useful and consistent data describing the posterior corneal surface.

There have also been reports of KCN evaluation with Orbscan. Auffarth and associates<sup>23</sup> studied 71 eyes of 38 KCN patients with a primary focus on quantitative parameters at vectorial location of the apex and the thinnest point in reference to the central cornea. Rao and associates<sup>35</sup> examined 60 eyes of KCN suspects with Orbscan II and videokeratography using Rabinowitz and Klyce/Maeda methods. They compared the mean values of thinnest optical pachymetry, anterior and posterior elevation values, of those patients with those of a group of 50 normal eyes.

Relative to previous studies, our study represents the most extensive analysis to date of Orbscan parameters with respect to distinguishing normal from keratoconic eyes. Most of the parameters studied showed significantly different mean values between the two groups. Many of these parameters, however, are interrelated and are not independent. Tables 3 and 5 show those parameters with the highest intragroup correlations in the normal and keratoconic groups, indicating redundancy in the information they provide. Some of these relationships are not surprising. For example, the dependence of I–S K3 and I–S K5, as well as SRAX3 and SRAX5, are expected because these pairs of parameters are describing the same curvature asymmetry at different radii. Other relationships are of more interest. The dependence between keratometric and tangential I–S differences in both the normal and KCN groups suggest that we need not include both types of maps

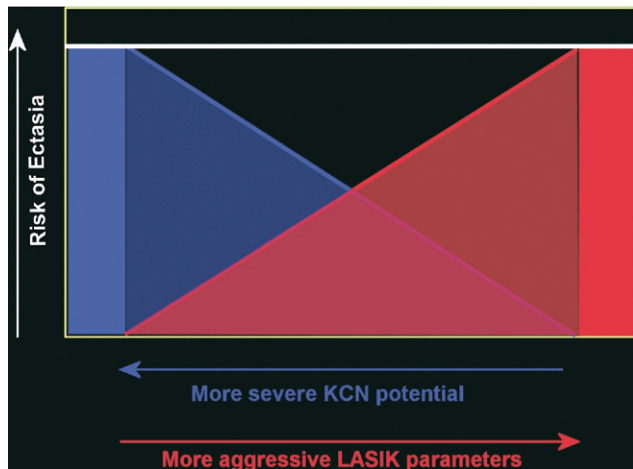


**FIGURE 3.** The post-laser in situ keratomileusis (LASIK) ectasia paradigm. Aggressiveness of LASIK parameters increases from left to right (higher ablation depths, thicker flaps, thinner residual beds). Severity of keratoconus (KCN) potential increases from right to left. On the extreme left of the graph is an eye with manifest KCN that is ectatic without any refractive surgery. On the extreme right of the graph is an entirely normal eye that received a very high correction with an extremely thin residual bed in which ectasia developed after LASIK. The risk of ectasia is a continuum between these two extremes. Better identification of forme fruste KCN and more restraint with LASIK parameters will narrow the window of eyes at risk.

when developing an algorithm to distinguish normal from keratoconic morphologic features.

Of more interest are the parameters in Tables 4 and 6. These parameters have the lowest intragroup correlations in the normal and KCN groups. This weak correlation, together with highly statistically significant differences between groups, indicates that these parameters, taken together, may provide the most value in distinguishing normal from keratoconic corneas. It is important to note that MPE and TOP are parameters that are not available with placido only-based topographic systems.

One cannot conclude from this study that any single parameter taken alone or in combination with others is sufficient to distinguish a normal from a pathologic cornea. Several limitations of this study deserve discussion. There are multiple possible settings for best-fit surfaces, location of map centers, and reference axes. In this study, magnitudes and axes were determined using the Orbscan IIz default settings: best-fit sphere using floating alignment, full corneal fit (e.g., using all data points out to 10 mm), and apex centration as determined by the Placido image. The full corneal fit default setting may lead to nonuniform best-fit spheres because some eyes have data points only out to 8 or 9 mm. In addition, other best-fit surfaces (e.g., aconic) and centration reference points (e.g., corrected apex using data from both Placido and elevation maps with surface rotation) are possible on the system. Future studies

should investigate these other settings to determine if they improve the ability to separate normal from keratoconic corneal morphologic features.

Future work will focus on the development of a logistical regression model to quantify probability of corneal pathologic status based on these parameters, similar to the Klyce/Maeda and KISA indices developed for anterior topographic systems.<sup>11–13,25,33</sup>

In conclusion, a paradigm clearly exists describing the risk of ectasia after refractive surgery (Figure 3). On the extreme left of the graph is an eye with manifest KCN that is ectatic without any refractive surgery. On the extreme right of the graph is an entirely normal cornea that received a very high correction with an extremely thin residual bed and in which ectasia developed after LASIK. The risk of ectasia is a continuum between these two extremes. Better identification of FFKCN and more restraint with LASIK parameters will narrow, but not eliminate, this window of corneas at risk.

---

THE AUTHORS INDICATE NO FINANCIAL SUPPORT OR FINANCIAL conflict of interest. Involved in the design of study (B.S., M.P.D., D.R.H.); conduct of study (B.S., M.P.D., D.R.H.); collection of data (B.S., M.P.D., D.R.H.); management of data (B.S., M.P.D., D.R.H.); statistical analysis (D.R.H.); analysis and interpretation of data (B.S., M.P.D., D.R.H.); preparation of the manuscript (B.S., M.P.D., D.R.H.); and review and approval of manuscript (B.S., M.P.D., D.R.H.).

The authors thank Fei Yu, PhD, The Jules Stein Eye Institute, University of California, Los Angeles, Los Angeles, California, for statistical consultation and assistance.

---

## REFERENCES

- Duffey RJ, Leaming D. US trends in refractive surgery: 2004 ISRS/AAO Survey. *J Refract Surg* 2005;21:742–748.
- Sugar A, Rapuano CJ, Culbertson WW, et al. Laser in situ keratomileusis for myopia and astigmatism: safety and efficacy. A report by the American Academy of Ophthalmology. *Ophthalmology* 2002;109:175–187.
- Twa MD, Nichols JJ, Joslin CE, et al. Characteristics of corneal ectasia after LASIK for myopia. *Cornea* 2004;23:447–457.
- Chiang RK, Park AJ, Rapuano CJ, Cohen EJ. Bilateral keratoconus after LASIK in a keratoconus patient. *Eye Contact Lens* 2003;29:90–92.
- Jabbur NS, Stark WJ, Green WR. Corneal ectasia after laser-assisted in situ keratomileusis. *Arch Ophthalmol* 2001;119:1714–1716.
- Fogla R, Rao SK, Padmanabhan P. Keratectasia in 2 cases with pellucid marginal corneal degeneration after laser in situ keratomileusis. *J Cataract Refract Surg* 2003;29:788–791.
- Randleman JB, Russell B, Ward MA, Thompson KP, Stulting RD. Risk factors and prognosis for corneal ectasia after LASIK. *Ophthalmology* 2003;110:267–275.
- Seiler T, Quurke AW. Iatrogenic keratectasia after LASIK in a case of forme fruste keratoconus. *J Cataract Refract Surg* 1998;24:1007–1009.

9. Bilgihan K, Ozdek SC, Konuk O, Akata F, Hasanreisoglu B. Results of photorefractive keratectomy in keratoconus suspects at 4 years. *J Refract Surg* 2000;16:438–443.
10. Malecaze F, Coulet J, Calvas P, Fournie P, Arne JL, Brodaty C. Corneal ectasia after photorefractive keratectomy for low myopia. *Ophthalmology* 2006;113:742–746.
11. Maeda N, Klyce SD, Smolek MK, Thompson HW. Automated keratoconus screening with corneal topography analysis. *Invest Ophthalmol Vis Sci* 1994;35:2749–2757.
12. Smolek MK, Klyce SD. Current keratoconus detection methods compared with a neural network approach. *Invest Ophthalmol Vis Sci* 1997;38:2290–2299.
13. Rabinowitz YS, Rasheed K. KISA% index: a quantitative videokeratography algorithm embodying minimal topographic criteria for diagnosing keratoconus. *J Cataract Refract Surg* 1999;25:1327–1335.
14. Guirao A. Theoretical elastic response of the cornea to refractive surgery: risk factors for keratectasia. *J Refract Surg* 2005;21:176–185.
15. Giledi O, Daya SM. Unexpected flap thickness in laser in situ keratomileusis. *J Cataract Refract Surg* 2003;29:1825–1826.
16. Amoils SP, Deist MB, Gous P, Amoils PM. Iatrogenic keratectasia after laser in situ keratomileusis for less than  $-4.0$  to  $-7.0$  diopters of myopia. *J Cataract Refract Surg* 2000;26:967–977.
17. Lifshitz T, Levy J, Klemperer I, Levinger S. Late bilateral keratectasia after LASIK in a low myopic patient. *J Refract Surg* 2005;21:494–496.
18. Ou RJ, Shaw EL, Glasgow BJ. Keratectasia after laser in situ keratomileusis (LASIK): evaluation of the calculated residual stromal bed thickness. *Am J Ophthalmol* 2002;134:771–773.
19. Wang JC, Hufnagel TJ, Buxton DF. Bilateral keratectasia after unilateral laser in situ keratomileusis: a retrospective diagnosis of ectatic corneal disorder. *J Cataract Refract Surg* 2003;29:2015–2018.
20. Wei RH, Lim L, Chan WK, Tan DT. Evaluation of Orbscan II corneal topography in individuals with myopia. *Ophthalmology* 2006;113:177–183.
21. Liu Z, Huang AJ, Pflugfelder SC. Evaluation of corneal thickness and topography in normal eyes using the Orbscan corneal topography system. *Br J Ophthalmol* 1999;83:774–778.
22. Modis L Jr, Langenbucher A, Seitz B. Evaluation of normal corneas using the scanning-slit topography/pachymetry system. *Cornea* 2004;23:689–694.
23. Auffarth GU, Wang L, Volcker HE. Keratoconus evaluation using the Orbscan Topography System. *J Cataract Refract Surg* 2000;26:222–228.
24. Wang M. Corneal topography in the wavefront era. A guide for clinical application. Thorofare, New Jersey: SLACK Inc, 2006:1–336.
25. Rabinowitz YS. Videokeratographic indices to aid in screening for keratoconus. *J Refract Surg* 1995;11:371–379.
26. Pallikaris IG, Papatzanaki ME, Stathi EZ, Frenschok O, Georgiades A. Laser in situ keratomileusis. *Lasers Surg Med* 1990;10:463–468.
27. Munnerlyn CR, Koons SJ, Marshall J. Photorefractive keratectomy: a technique for laser refractive surgery. *J Cataract Refract Surg* 1988;14:46–52.
28. Binder PS, Lindstrom RL, Stulting RD, et al. Keratoconus and corneal ectasia after LASIK. *J Cataract Refract Surg* 2005;31:2035–2038.
29. Holland SP, Srivannaboon S, Reinstein DZ. Avoiding serious corneal complications of laser-assisted in situ keratomileusis and photorefractive keratectomy. *Ophthalmology* 2000;107:640–652.
30. Kohnen T. Iatrogenic keratectasia: current knowledge, current measurements. *J Cataract Refract Surg* 2002;28:2065–2066.
31. McLeod SD, Kislak TA, Caro NC, McMahon TT. Iatrogenic keratoconus: corneal ectasia following laser in situ keratomileusis for myopia. *Arch Ophthalmol* 2000;118:282–284.
32. Schmitt-Bernard CF, Lesage C, Arnaud B. Keratectasia induced by laser in situ keratomileusis in keratoconus. *J Refract Surg* 2000;16:368–370.
33. Klyce SD, Smolek MK, Maeda N. Keratoconus detection with the KISA% method—another view. *J Cataract Refract Surg* 2000;26:472–474.
34. Cairns G, McGhee CN. Orbscan computerized topography: attributes, applications, and limitations. *J Cataract Refract Surg* 2005;31:205–220.
35. Rao SN, Raviv T, Majmudar PA, Epstein RJ. Role of Orbscan II in screening keratoconus suspects before refractive corneal surgery. *Ophthalmology* 2002;109:1642–1646.



### **Biosketch**

Baris Sonmez, MD, received his MD from the Hacettepe University of Ankara, Turkey, in 1999. Dr Sonmez pursued his residency training in Ophthalmology at the same institution in 2003. He completed his Fellowship in cornea and refractive surgery at the Jules Stein Eye Institute, Los Angeles, in 2006. Dr Sonmez is currently a Assistant Professor of Ophthalmology at the Ondokuzmayis University of Samsun, Turkey. Dr Sonmez's chief research interests include molecular genetics of corneal dystrophies and corneal ectasia.



### **Biosketch**

D. Rex Hamilton, MD, MS, received his doctor of medicine degree at the University of California, Irvine, and did his residency training at the Jules Stein Eye Institute. He then completed a one-year fellowship in cornea/anterior segment surgery at Minnesota Eye Consultants under the directorship of Dr Richard Lindstrom. Dr Hamilton serves on the AAO Preferred Practice Pattern Committee for Refractive Surgery, a committee which sets standards of care in refractive surgery. His research interests include corneal biomechanics, new keratorefractive surgical technologies, phakic intraocular lenses, and accommodative intraocular lenses.